JOURNAL OF THERMOPHYSICS AND HEAT TRANSFER
Vol. 23, No. 3, July–September 2009

Raman Scattering Characterization of Transparent Thin Film for Thermal Conductivity Measurement

Shuo Huang,* Xiaodong Ruan,† Jun Zou,‡ Xin Fu,† and Huayong Yang†
Zhejiang University, 310027 Hangzhou, People's Republic of China

DOI: 10.2514/1.40976

The Raman scattering method is a noncontact and nondestructive method for film thermal conductivity measurement. However, the original Raman scattering method cannot calculate the thermal conductivity of thin transparent films with submicrometer- or nanometer-scale thickness. An analytical heat transfer model has been built to extend the original Raman scattering method to thin transparent films with submicrometer- or nanometer-scale thickness. Experiments were performed using the extended method to measure the thermal conductivity of silicon dioxide films with submicrometer-scale thickness. The interface thermal resistance between the silicon dioxide film and the silicon substrate was also obtained. The experimental results are consistent with reported data.

Nomenclature

$J_1(\lambda)$	=	first-order Bessel function
k_a	=	thermal conductivity of the air
k_{eff}	=	effective thermal conductivity of the film
k_f	=	thermal conductivity of the film
k_s	=	thermal conductivity of the substrate
Nu	=	local Nusselt number
P	=	laser power
R_i	=	film/substrate interface area thermal resistance
$\hat{t}$	=	average local temperature of the film surface
t_f	=	local temperature of the film at the place that the laser beam irradiates
t_i	=	local temperature of the interface between the film and the substrate
t_s	=	local temperature of the substrate
t_∞	=	room temperature
$2R_0$	=	laser beam diameter
α	=	local heat transfer coefficient, $Nu(k_a/2R_0)$
ΔT	=	local temperature rise
δ	=	film thickness

Subscripts

a	=	air
eff	=	effective
f	=	film
i	=	interface
s	=	substrate
∞	=	far field

Introduction

RECENTLY, with the development of microelectromechanical system (MEMS) technology, the research of the thermal-effect microsystems (TEMS) has attracted much attention. Heat transfer plays an important role in the performance of the TEMS. The operating principles of typical TEMS, such as infrared detectors and thermal flow sensors, require a reliable thermal insulation of the sensing elements from the silicon substrate. This improves the measurement accuracy by reducing the impact of heat dissipation in the silicon substrate [1]. In TEMS, silicon dioxide film is commonly used as the thermal insulating layer, due to its low thermal conductivity and simple fabrication process [1,2]. Silicon dioxide film is also widely used as the electrical insulating layer in the integrated circuits (ICs), and the thermal characteristics of silicon dioxide film would greatly impact the heat dissipation of the chips. To evaluate the heat dissipation in silicon dioxide film, it is very important to investigate its thermal conductivity. A measurement method is then required to obtain the thermal conductivity of silicon dioxide film for the research of both TEMS' thermally insulated structure and heat dissipation in ICs [3].

Several methods for measuring film thermal conductivity have been reported, such as the steady-state method [4], 3ω method [5], photoacoustic and photothermal methods [6,7], thermal microscopy method [3], etc. Both the steady-state and 3ω methods require depositing a metal layer on the measured film, which may risk damaging and changing the properties of the measured film. Photoacoustic and photothermal methods are noncontact but indirect methods requiring extensive data analysis. The thermal microscopy method uses a probe as a key component, but the fabrication process of the probe is very complicated.

Raman scattering spectroscopy has been applied to a very wide range of materials such as semiconductors, diamond films, ceramics, polymer composites, etc. The high spatial resolution of Raman scattering spectroscopy enables this technique to be applied to microphysical features. [8] Recently, Raman scattering has been increasingly used to study the local mechanical stress [9–12], temperature rise [13,14], and thickness [8] in IC and MEMS devices. Stress or temperature distribution varies significantly within the volume of material, which contributes to the detected Raman signal.

Perichon et al. [15] presented a thermal conductivity measurement method with Raman scattering spectroscopy in 1999. It is a noncontact and nondestructive method. To apply this Raman scattering method, however, the thickness of the film is required to be at least one order larger than the laser diameter. But the laser beam diameter of the Raman scattering device is from several to tens of micrometers, which means that this method cannot be applied directly to the thin film with submicrometer- or nanometer-scale thickness.

To extend the Raman scattering method to the thermal conductivity measurement of transparent thin films with submicrometer- or nanometer-scale thickness, an analytical heat transfer model was developed. The model describes the laser-induced heat transfer process inside a sample that is composed of a transparent thin film and a thick substrate. By using the extended Raman scattering method, experiments were performed to measure the thermal conductivity of submicrometer- and nanometer-scale-thickness silicon

Received 13 September 2008; revision received 17 March 2009; accepted for publication 26 March 2009.

*State Key Laboratory of Fluid Power Transmission and Control.
†Professor, State Key Laboratory of Fluid Power Transmission and Control.
‡Associate Professor, State Key Laboratory of Fluid Power Transmission and Control (Corresponding Author).

dioxide films. The interface thermal resistance between silicon dioxide film and silicon substrate was also obtained.

Extension of the Raman Scattering Method

Raman Scattering Method

Consider a sample consisting of thick substrate and a film above the substrate. The laser beam of the Raman scattering device is focused on the sample and causes the local heating on the sample surface, as shown in Fig. 1. The heat absorbed by the sample yields a temperature distribution within the film when the film thickness is at least one order larger than the laser beam diameter and the distribution of the isotherms is quasi-hemispherical. In this case, the heat transfer across the film/substrate interface is negligible [15]. There is a relationship between the local temperature rise and the laser beam power [16]:

$$\Delta T = \frac{2P}{\pi K_f d} \quad \text{or } K_f = \frac{2P}{\pi \Delta T d} \tag{1}$$

where ΔT is the local temperature rise, P is the laser power, K_f is the film thermal conductivity, d is the laser beam diameter, and

$$\Delta T = T_f - T_s \tag{2}$$

where T_f is the local temperature of the film at the place that the laser beam irradiates, and T_s is the substrate temperature. If P, T_s, and d are already known, then the film thermal conductivity K_f can be obtained when T_f is known.

To get T_f, Raman scattering spectroscopy is used to get the Raman spectra of the sample at different temperatures. The peak position of the Raman spectrum shifts as the sample temperature changes. First, calibrate the relationship between the sample temperature and the Raman peak position. Second, use the laser beam with power P in room temperature to get the corresponding Raman peak position. With the calibrated relationship, the local temperature T_f induced by laser beam with power P can be found. Finally, the film thermal conductivity k_f can be obtained by Eq. (1).

Only when the film thickness of the sample is at least one order larger than the laser beam diameter is the Raman scattering method applicable. When the film thickness is large enough (e.g., one order larger than the laser beam diameter), the heat created by the laser beam will transfer mostly within the film, then it can be assumed that the thermal conductivity obtained by the Raman scattering method exactly indicates the thermal characteristic of the film. The laser beam diameter of the Raman scattering spectroscopy device, however, is from several micrometers to tens of micrometers, which means that the film thickness of the sample has to be at least tens of micrometers to be applied with the Raman scattering method.

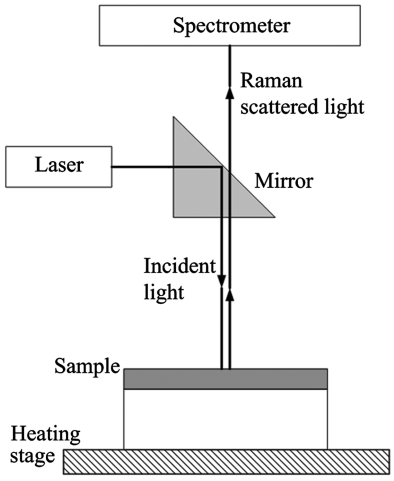

Fig. 1 Schematic of the film thermal conductivity measurement method based on Raman scattering spectroscopy. A local heating is created within the film by the laser beam, including quasi-hemispherical isotherms.

Extension of the Raman Scattering Method

Figure 2 shows a Gaussian laser beam irradiating a sample that consists of a thick substrate and a transparent thin film. The film thickness δ is of submicrometer or nanometer scale, and it is smaller than the diameter of the laser beam, $2R_0$. The center of the laser beam on the film sample surface is taken as the origin of the cylindrical coordinate system (r and z).

The intensity of the Gaussian laser beam is

$$f(r) = \frac{2P}{\pi R_0^2} \exp\left(-\frac{2r^2}{R_0^2}\right) \tag{3}$$

where P is the power of the laser beam, and r_0 is the radius at which the laser beam intensity is e^{-2} times its maximum value.

If the film is opaque, a shallow heating will be induced by the laser beam on the film surface; this process has been described in several studies [1,17,18]. But in the case of the transparent film, the shallow heating will be on the interface between the transparent thin film and the substrate. In this approximate analysis, it is assumed that the laser beam power is completely absorbed by the sample at the interface [15]. There are two kinds of heat transfer in the sample: 1) heat transfer inside the film and the substrate by conduction and 2) heat transfer from the thin film surface to the air by free convection. Assuming that the film thickness is much less than the substrate thickness (i.e., the substrate is relatively an infinite half-plane), then,

$$\frac{\partial^2 t_f(r,z)}{\partial r^2} + \frac{1}{r}\frac{\partial t_f(r,z)}{\partial r} + \frac{\partial^2 t_f(r,z)}{\partial z^2} = 0 \tag{4}$$

$$\frac{\partial^2 t_s(r,z)}{\partial r^2} + \frac{1}{r}\frac{\partial t_s(r,z)}{\partial r} + \frac{\partial^2 t_s(r,z)}{\partial z^2} = 0 \tag{5}$$

where $t_f(r,z)$ is the temperature in the film and $t_s(r,z)$ is the temperature in the substrate.

Because of the heat flux and temperature continuity, the boundary conditions are

$$t_f(r,z) = t_s(r,z) \quad \text{at } z = \delta \tag{6}$$

$$k_{\text{eff}}\frac{\partial t_f(r,z)}{\partial z} + k_s\frac{\partial t_s(r,z)}{\partial z} = -f(r) = -\frac{2P}{\pi R_0^2}\exp\left(-\frac{R_0^2\lambda^2}{8}\right) \quad \text{at } 0 < r < R_0, \qquad z = \delta \tag{7}$$

$$k_{\text{eff}}\frac{\partial t_f(r,z)}{\partial z} = \alpha[t_f(r,z) - t_\infty] \quad \text{at } 0 < r < R_0, \qquad z = 0 \tag{8}$$

where k_{eff} is the effective thermal conductivity of the transparent thin film, composed of the intrinsic thermal conductivity of the film and the interface thermal resistance, k_s is the thermal conductivity of the substrate, k_a is the thermal conductivity of the air, t_∞ is the room temperature, and α is the local heat transfer coefficient, which can be calculated according to the work of Fishenden and Saunders [19].

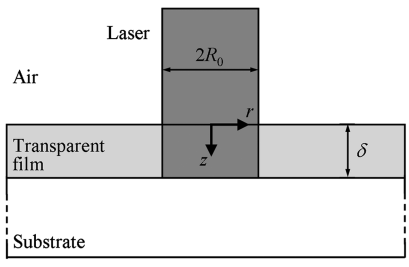

Fig. 2 Film and substrate in cylindrical coordinate system (r and z).

It is assumed that as $(r^2+z^2)^{1/2}\to\infty$ and $t_s(r,z)\to 0$.
By taking the Hankel transform of order zero, Eqs. (4–8) turn to

$$\frac{d^2T_f(\lambda,z)}{dz}-\lambda^2T_f(\lambda,z)=0 \tag{9}$$

$$\frac{d^2T_s(\lambda,z)}{dz}-\lambda^2T_s(\lambda,z)=0 \tag{10}$$

$$T_f(\lambda,\delta)=T_s(\lambda,\delta) \tag{11}$$

$$k_{\text{eff}}\frac{\partial T_f(\lambda,\delta)}{\partial z}+k_s\frac{\partial T_s(\lambda,\delta)}{\partial z}=-\frac{P}{2\pi}\exp\left(-\frac{R_0^2\lambda^2}{8}\right) \tag{12}$$

$$k_{\text{eff}}\frac{\partial T_f(\lambda,0)}{\partial z}=\alpha T_f(\lambda,0) \tag{13}$$

The transformed temperature will have the form

$$T_f(\lambda,z)=A(\lambda)\exp(\lambda z)+B(\lambda)\exp(-\lambda z) \tag{14}$$

$$T_s(\lambda,z)=C(\lambda)\exp(\lambda z)+D(\lambda)\exp(-\lambda z) \tag{15}$$

where

$$A(\lambda)=\frac{P}{2\pi}\cdot\frac{(\lambda k_{\text{eff}}+\alpha)\exp(-(R_0^2\lambda^2/8))}{\lambda[(k_s-k_{\text{eff}})(\lambda k_{\text{eff}}+\alpha)\exp(\lambda\delta)+(k_s+k_{\text{eff}})(\lambda k_{\text{eff}}-\alpha)\exp(-\lambda\delta)]} \tag{16}$$

$$B(\lambda)=\frac{P}{2\pi}\cdot\frac{(\lambda k_{\text{eff}}-\alpha)\exp(-(R_0^2\lambda^2/8))}{\lambda[(k_s-k_{\text{eff}})(\lambda k_{\text{eff}}+\alpha)\exp(\lambda\delta)+(k_s+k_{\text{eff}})(\lambda k_{\text{eff}}-\alpha)\exp(-\lambda\delta)]} \tag{17}$$

$$C(\lambda)=0 \tag{18}$$

$$D(\lambda)=\frac{P}{2\pi}\cdot\frac{[(\lambda k_{\text{eff}}-\alpha)+(\lambda k_{\text{eff}}+\alpha)\exp(2\lambda\delta)]\exp(-(R_0^2\lambda^2/8))}{\lambda[(k_s-k_{\text{eff}})(\lambda k_{\text{eff}}+\alpha)\exp(\lambda\delta)+(k_s+k_{\text{eff}})(\lambda k_{\text{eff}}-\alpha)\exp(-\lambda\delta)]} \tag{19}$$

By taking the inverse Hankel transform, the temperature of the interface between the thin film and the thick substrate is

$$t_f(r,\delta)=\int_0^\infty \lambda T_f(\lambda,\delta)J_0(\lambda r)\mathrm{d}\lambda \tag{20}$$

where $J_0(\lambda r)$ is the zero-order Bessel function.

The average temperature of the thin film surface is

$$\begin{aligned}\hat{t}&=\frac{1}{\pi R_0^2}\int_0^{R_0}t_f(r,0)2\pi r\mathrm{d}r\\&=\frac{2}{R_0^2}\int_0^\infty\lambda T_f(\lambda,0)\left[\int_0^{R_0}J_0(\lambda r)r\mathrm{d}r\right]\mathrm{d}\lambda\\&=\frac{2}{R_0}\int_0^\infty T_f(\lambda,0)J_1(\lambda R_0)\mathrm{d}\lambda\\&=\frac{2Pk_{\text{eff}}}{\pi R_0(k_s+k_{\text{eff}})}\\&\times\int_0^\infty\left[\frac{1}{\frac{k_s-k_{\text{eff}}}{k_s+k_{\text{eff}}}(\bar{\lambda}+\frac{R_0\alpha}{k_{\text{eff}}})\exp(\frac{\delta}{R_0}\bar{\lambda})+(\bar{\lambda}-\frac{R_0\alpha}{k_{\text{eff}}})\exp(-\frac{\delta}{R_0}\bar{\lambda})}\right.\\&\left.\cdot\exp\left(-\frac{\bar{\lambda}^2}{8}\right)\cdot\frac{1}{\bar{\lambda}}\cdot J_1(\bar{\lambda})\right]\mathrm{d}\bar{\lambda}\end{aligned} \tag{21}$$

where $\bar{\lambda}=R_0\lambda$.

If the thermal conductivity of the film is much less than that of the substrate and the thickness of thin film is much less than the diameter of the laser beam, then

$$\begin{aligned}\hat{t}&=\frac{Pk_{\text{eff}}}{\pi R_0(k_s+k_{\text{eff}})((\delta\alpha/k_{\text{eff}})+1)}\int_0^\infty\exp\left(-\frac{\bar{\lambda}^2}{8}\right)\cdot\frac{1}{\bar{\lambda}}\cdot J_1(\bar{\lambda})\mathrm{d}\bar{\lambda}\\&=\frac{[I_0(1)+I_1(1)]Pk_{\text{eff}}}{\sqrt{2\pi}eR_0(k_s+k_{\text{eff}})((\delta\alpha/k_{\text{eff}})+1)}\end{aligned} \tag{22}$$

where $I_0(x)$ is the zero-order modified Bessel function of the first kind, and $I_1(x)$ is the first-order modified Bessel function of the first kind.

Carslaw and Jaeger [20] obtained the expression of thermal resistance for the case of a semi-infinite half-space. Because the heat created by the laser transfers in the film and the substrate by conduction at the first place, then

$$P=4R_0k_s(t_i-t_\infty)+\frac{\pi R_0}{\delta}k_{\text{eff}}(t_i-\hat{t}) \tag{23}$$

The first term in Eq. (23) is the heat in the substrate due to the thermal resistance, and the second term indicates the heat in the film. The micro-Raman spectroscopy device could be used to find the local temperature of the interface between the film and substrate, and then the effective thermal conductivity of the film can be obtained by Eq. (23).

Experiments

Sample Preparation and Experimental Setup

The silicon dioxide film samples were prepared by depositing the silicon dioxide films on the silicon substrates with the magnetron sputtering device at 100°C. The silicon substrate was *p*-type, <100>-oriented, with a thickness of 525 μm and thermal conductivity of 157 $\mathrm{W\cdot m^{-1}\cdot K^{-1}}$. The thickness of the silicon dioxide films was measured using a Kosaka SE3500 profile meter with an accuracy of 5 nm.

The micro-Raman spectroscopy device used in our test was an Almega (Thermo Nicolet Co.) with an Olympus BX50 microscope. The measurement range of the Raman spectrum was 100–4000 $\mathrm{cm^{-1}}$. An $\mathrm{Ar^+}$-ion laser with a wavelength of 514 nm was used in our experiments. The power distribution of the laser beam has a Gaussian nature [21]; however, it can be assumed that the constant mean value of the laser beam diameter is 5 μm.

Thermal Conductivity Measurement of Silicon Dioxide Films

In this section, we present the process of thermal conductivity measurement of sample 1, for which the thickness of silicon dioxide film is 200 nm. A detailed experimental process has been described in several studies [1,15,18]. Sample 1 was heated to different temperatures from 100 to 500°C with an interval of 100°C by using

the heating stage with an accuracy of 1°C to calibrate the relationship between the sample temperature and its Raman peak position. Because the thermal conductivity of silicon substrate falls off rapidly as its temperature rises [22], the heating stage was held for 1 min at each temperature to ensure that the film was thoroughly heated. Then the Raman spectrum was acquired at each temperature; the power of the laser beam was 1.1 mW, and the acquisition time was longer than 12 s. Note that a low-power laser beam was used in the calibration to avoid inducing an additional temperature rise. The Raman peak positions of sample 1 were marked, as shown in Fig. 3. The relationship between the temperature and the Raman peak position of sample 1 could then be calibrated, as shown in Fig. 4.

Figure 4 indicates the near-linear relationship between the temperature and the Raman peak position of the tested sample: the Raman peak position decreases as the temperature rises. A similar linear relationship was reported by Balkanski et al. [23].

A high-power laser beam with $P = 4$ mW was focused on sample 1 at room temperature, and the corresponding Raman spectrum was acquired. The uncertainty of the Raman peak position was estimated to be ± 0.25 cm^{-1}, due to the resolution of the micro-Raman spectroscopy device. The Raman spectrum quality could be improved by enhancing the acquisition time to be longer than 12 s, enabling the Raman peak position to be acquired more accurately. By using the value of the Raman peak position induced by high-power laser irradiation, the corresponding temperature value was determined in Fig. 4. This laser-induced temperature is the average temperature of the interface between the transparent thin film and the thick substrate. The thickness of sample 1 was much larger than the laser beam diameter $2R_0$, the silicon dioxide film thickness δ was much smaller than the silicon substrate thickness and the laser beam diameter $2R_0$, and the thermal conductivity of silicon dioxide film k_{eff} reported in studies [3,24] was much smaller than the thermal conductivity of silicon substrate k_s, which means that the assumptions of the extension process were all met. So the effective thermal conductivity of silicon dioxide film k_{eff} can be obtained by Eq. (23), as shown in Fig. 5. In our experiment, we assume that the heat loss by conduction in the air is negligible, because the thermal conductivity of the air is 0.0026 W · cm^{-1} · K^{-1} at 300 K. The heat loss caused by thermal radiation, which is proportional to the fourth power of the sample temperature, is strong when the temperature is higher than 1000 K. The temperature of the samples in our experiment is, however, usually much less than 1000 K.

Figure 5 shows an obvious decrease in the effective thermal conductivity of the thin film with the decrease in the thickness of the silicon dioxide film. The decrease in the effective thermal conductivity is less than 1 order of magnitude and is similar to published results [25,26]. There are three possible reasons for this observed decrease in effective thermal conductivity. The first is that phonon boundary scattering of the thermal carriers reduces the thermal conductivity of the thin film. We believe that phonons with mean free paths do not cause a significant decrease of film thermal conductivity at room temperature, as claimed by many authors [27–29]. The second is that the microstructure and stoichiometry of the thin film changes. Internal defects such as dislocation and cracks can influence the heat transport in thin film. Burzo et al. [26] suspected that the difference in the microstructure of sputtered silicon dioxide film is responsible for the decrease in the effective thermal conductivity. The third possible reason is that thermal resistance at the interface between the thin film and the substrate can affect the effective thermal conductivity of thin film. A plausible hypothesis is the presence of a porous layer at the interface which results in heat transport reduction through the interface. To calculate the interface thermal resistance, a 1-D heat flow analysis is applicable, as

$$\frac{\delta}{k_{\text{eff}}} = \frac{\delta}{k_f} + R_i \tag{24}$$

where k_f is the intrinsic thermal conductivity of thin film and R_i is the interface thermal resistance.

Equation (24) implies a plot of δ/k_{eff} vs δ, which has a slope of $1/k_f$ and an intercept of R_i, as shown in Fig. 6.

As shown in Fig. 6, for silicon dioxide film of thickness $\leq$ 300 nm, a straight line can be fitted to give the value of k_f and R_i. An intrinsic film thermal conductivity of (1.26 ± 0.09) W · m^{-1} · K^{-1} can be found in Fig. 6 for silicon dioxide film. This value is in agreement with the published data. For example, Burzo et al. [26] reported a thermal conductivity of 1.27 W · m^{-1} · K^{-1} for thermally grown silicon dioxide film and 1.05 W · m^{-1} · K^{-1} for ion-beam-sputtered silicon dioxide film; Kato and Hatta [30] reported a thermal conductivity of (1.24 ± 0.04) W · m^{-1} · K^{-1} using a thermoreflectance method. The interface thermal resistance between silicon dioxide film and substrate is $(4.49 \pm 0.38) \times 10^{-8}$ m^2 · KW^{-1}. This also has some similarity with the value of 2.58×10^{-8} m^2 · KW^{-1} for ion-beam-sputtered silicon dioxide film on silicon

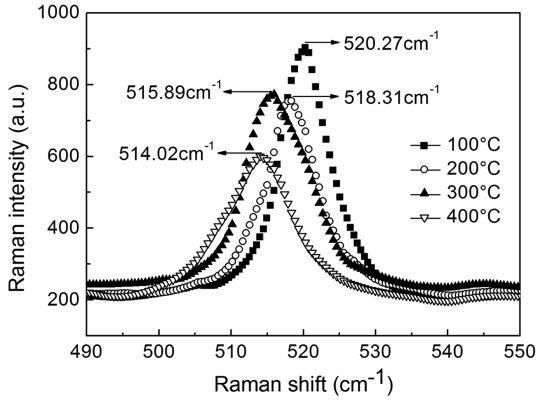

Fig. 3 Raman spectra and peak positions of sample 1 at four different temperatures of 100, 200, 300, and 400°C.

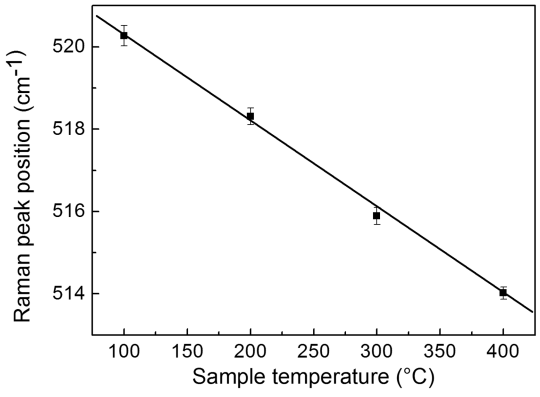

Fig. 4 Raman peak position vs temperature of sample 1 at low laser power $P = 1.1$ mW.

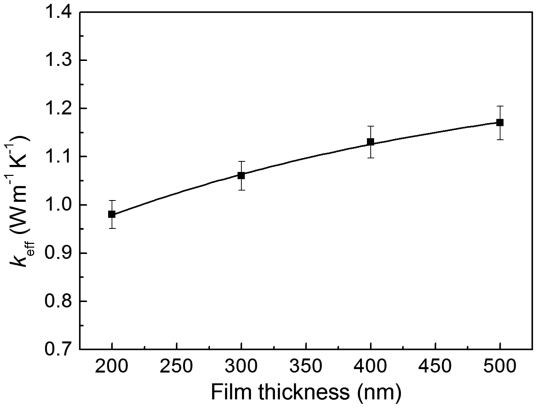

Fig. 5 Measurement results of the extended Raman scattering method, variation of effective thermal conductivity of thin film with thickness for silicon dioxide film.

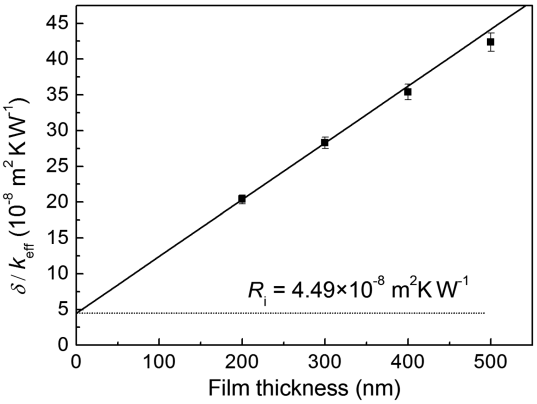

Fig. 6 Variation of effective thermal resistance with thickness for silicon dioxide films.

substrate according to Burzo et al. [26]. Considering the impact of different thin film fabrication processes, some small differences in the measured thermal conductivity data are inevitable.

The main random error of the Raman scattering method is estimated to be 15% because of the ± 0.25 cm^{-1} uncertainty on the Raman peak position. However, by enhancing the acquisition time, the Raman spectra quality can be improved. Systematic errors associated with the effective laser beam diameter and heat radiation and convection will be taken into account in future, more quantitative, studies.

In addition to using the Raman peak position, a new technique was presented by Beechem et al. [31] to obtain the local temperature rise. This new technique uses the dependency of the Raman full width at half-maximum on the temperature to negate the measurement uncertainty of Raman peak position technique induced by the stress inside the film sample. We also used this technique to obtain the local temperature of the interface between the film and the substrate. The resulting thermal conductivity of silicon dioxide film is $1.17\ W \cdot m^{-1} \cdot K^{-1}$, and the interface thermal resistance between silicon dioxide film and substrate is $3.17 \times 10^{-8}\ m^2 \cdot KW^{-1}$.

Conclusions

An analytical model is presented to describe the heat transfer process in a submicrometer- or nanometer-scale-thickness transparent thin film on a thick substrate. This enables the extension of the micro- Raman method to thermal conductivity measurements of transparent thin films with submicrometer- or nanometer-scale thickness. The extended micro-Raman method has been applied to the intrinsic thermal conductivity measurement of silicon dioxide films with submicrometer-scale thickness. The interface thermal resistance between silicon dioxide film and silicon substrate was also obtained. The obtained values were in agreement with previously published data thereby validating our work. The extended micro-Raman method is a noncontact, nondestructive, and easy method for the measurement of thermal conductivity of both bulk material and transparent thin film. It provides new opportunities for research into both TEMS thermally insulated structures and heat dissipation in IC.

Acknowledgments

This work is supported by the International S&T Cooperation Program of China (2008DFR70410) and the Zhejiang Provincial Natural Science Foundation of China (R105008).

References

[1] Perichon, S., Lysenko, V., Roussel, Ph., Remaki, B., Champagnon, B., Barbier, D., and Pinard, P., "Technology and Micro-Raman Characterization of Thick Meso-Porous Silicon Layers for Thermal Effect Microsystems," *Sensors and Actuators A (Physical)*, Vol. 85, Nos. 1–3, 2000, pp. 335–339. doi:10.1016/S0924-4247(00)00327-7

[2] Roh, S. C., Choi, Y. M., and Kim, S. Y., "Sensitivity Enhancement of a Silicon Micro-Machined Thermal Flow Sensor," *Sensors and Actuators A (Physical)*, Vol. 128, No. 1, Mar. 2006, pp. 1–6. doi:10.1016/j.sna.2005.05.007

[3] Callard, S., Tallarida, G., Borghesi, A., and Zanotti, L., "Thermal Conductivity of SiO2 Films by Scanning Thermal Microscopy," *Journal of Non-Crystalline Solids*, Vol. 245, Nos. 1–3, 1999, pp. 203–209. doi:10.1016/S0022-3093(98)00863-1

[4] Zhang, X., and Grigoropoulos, C. P., "Thermal Conductivity and Diffusivity of Free-Standing Silicon Nitride Thin Films," *Review of Scientific Instruments*, Vol. 66, No. 2, 1995, p. 1115. doi:10.1063/1.1145989

[5] Yamane, T., Nagai, N., Katayama, S., and Todoki, M., "Measurement of Thermal Conductivity of Silicon Dioxide Thin Films Using a 3ω Method," *Journal of Applied Physics*, Vol. 91, June 2002, p. 9772. doi:10.1063/1.1481958

[6] Swimm, R. T., "Photoacoustic Determination of Thin-Film Thermal Properties," *Applied Physics Letters*, Vol. 42, No. 11, 1983, p. 955. doi:10.1063/1.93812

[7] Yacoubi, N., and Alibert, C., "Determination of Very Thin Semiconductor Layer Thickness by a Photothermal Method," *Journal of Applied Physics*, Vol. 69, June 1991, p. 8310. doi:10.1063/1.347441

[8] Wu, X., Yu, J., Ren, T., and Liu, L., "Micro-Raman Measurement of Thickness in Microelectromechanical Silicon Structures," *Journal of Micromechanics and Microengineering*, Vol. 17, No. 6, 2007, pp. 1114–1120. doi:10.1088/0960-1317/17/6/003

[9] Wolf, I. De, "Stress Measurements in Si Microelectronics Devices Using Raman Spectroscopy," *Journal of Raman Spectroscopy*, Vol. 30, Oct. 1999, pp. 877–883. doi:10.1002/(SICI)1097-4555(199910)30:10<877::AID-JRS464>3.0.CO;2-5

[10] Senez, V., Armigliato, A., and Wolf, I. De, "Strain Determination in Silicon Microstructures by Combined Convergent Beam Electron Diffraction, Process Simulation, and Micro-Raman Spectroscopy," *Journal of Applied Physics*, Vol. 94, Nov. 2003, p. 5574. doi:10.1063/1.1611287

[11] Srikar, V. T., Swan, A. K., Unlu, M. S., Goldberg, B. B., and Spearing, S. M., "Micro-Raman Measurement of Bending Stresses in Micromachined Silicon Flexures," *Journal of Microelectromechanical Systems*, Vol. 12, Dec. 2003, p. 779. doi:10.1109/JMEMS.2003.820280

[12] Kinnell, P. K., Gardiner, D. J., Bowden, M., Craddock, R., and Ward, M. C. L., "Characterization of a Micro-Engineered Selective Strain-Coupling Structure Using Raman Spectroscopy," *Journal of Micromechanics and Microengineering*, Vol. 15, Feb. 2005, pp. 807–811. doi:10.1088/0960-1317/15/4/019

[13] Cui, J. B., Amtmann, K., Ristein, J., and Ley, L., "Noncontact Temperature Measurements of Diamond by Raman Scattering Spectroscopy," *Journal of Applied Physics*, Vol. 83, June 1998, p. 7929. doi:10.1063/1.367972

[14] Serrano, J. R., Phinney, L. M., and Kearney, S. P., "Micro-Raman Thermometry of Thermal Flexure Actuators," *Journal of Micromechanics and Microengineering*, Vol. 16, No. 7, 2006, pp. 1128–1134. doi:10.1088/0960-1317/16/7/004

[15] Perichon, S., Lysenko, V., Remaki, B., Barbier, D., and Champagnon, B., "Measurement of Porous Silicon Thermal Conductivity by Micro-Raman Scattering," *Journal of Applied Physics*, Vol. 86, No. 8, 1999, p. 4700. doi:10.1063/1.371424

[16] McDonald, F., and Wetsel, G. C., "Theory of Photothermal and Photoacoustic Effects in Condensed Matter," *Physical Acoustics*, edited by W. P. Manson, Academic Press, New York, Vol. 18, 1998, p. 167.

[17] Huang, S., Ruan, X. D., Fu, X., and Yang, H. Y., "Measurement of the Thermal Transport Properties of Dielectric Thin Films Using the Micro-Raman Method," *Journal of Zhejiang University (Science)*, Vol. 10, No. 1, 2009, pp. 7–16. doi:10.1631/jzus.A0820493

[18] Huang, S., Ruan, X. D., Zou, J., Fu, X., and Yang, H. Y., "Thermal Conductivity Measurement of Submicrometer-Scale Silicon Dioxide Films by an Extended Micro-Raman Method," *Microsystem Technologies*, in Press.doi:10.1007/s00542-009-0824-3

[19] Fishenden, M., and Saunders, O. A., *An Introduction to Heat Transfer*, Clarendon, Oxford, 1950.

[20] Carslaw, H. S., and Jaeger, J. C., *Conduction of Heat in Solids*, 2nd ed., Oxford Univ. Press, London, 1959.

[21] Lax, M., "Temperature Rise Induced by a Laser Beam," *Journal of*

Applied Physics, Vol. 48, Dec. 1977, p. 3919.
doi:10.1063/1.324265

[22] Joshi, Y. P., Tiwari, M. D., and Verma, G. S., "Role of Four-Phonon Processes in the Lattice Thermal Conductivity of Silicon from 300 to 1300°K," *Physical Review B*, Vol. 1, No. 2, 1970, pp. 642–646.
doi:10.1103/PhysRevB.1.642

[23] Balkanski, M., Wallis, R. F., and Haro, E., "Anharmonic Effects in Light Scattering Due to Optical Phonons in Silicon," *Physical Review B*, Vol. 28, No. 4, 1983, pp. 1928–1934.
doi:10.1103/PhysRevB.28.1928

[24] Lee, S. M., Cahill, D. G., and Allen, T. H., "Thermal Conductivity of Sputtered Oxide Films," *Physical Review B*, Vol. 52, No. 1, 1995, pp. 253–257.
doi:10.1103/PhysRevB.52.253

[25] Lee, S. M., and Cahill, D. G., "Heat Transport in Thin Dielectric Films," *Journal of Applied Physics*, Vol. 81, No. 6, Mar. 1997, pp. 2590–2595.
doi:10.1063/1.363923

[26] Burzo, M. G., Komarov, P. L., and Raad, P. E., "Thermal Transport Properties of Gold-Covered Thin-Film Silicon Dioxide," *IEEE Transactions on Components and Packaging Technologies*, Vol. 26, No. 1, 2003, pp. 80–88.
doi:10.1109/TCAPT.2003.811467

[27] Love, M. S., and Anderson, A. C., "Estimate of Phonon Thermal Transport in Amorphous Materials Above 50 k," *Physical Review B*, Vol. 42, No. 3, 1990, pp. 1845–1847.
doi:10.1103/PhysRevB.42.1845

[28] Goodson, K. E., Flik, M. I., Su, L. T., and Antoniadis, D. A., "Prediction and Measurement of Thermal Conductivity of Amorphous Dielectric Layers," *Journal of Heat Transfer*, Vol. 116, No. 2, 1994, pp. 317–323.
doi:10.1115/1.2911402

[29] Cahill, D. G., "Heat Transport in Dielectric Thin Films and at Solid-Solid Interfaces," *Microscale Energy Transport*, Taylor & Francis, Washington, D.C., 1998, pp. 108–109.

[30] Kato, R., and Hatta, I., "Thermal Conductivity Measurement of Thermally-Oxidized SiO_2 Films on a Silicon Wafer Using a Thermoreflectance Technique," *International Journal of Thermophysics*, Vol. 26, No. 1, 2005, pp. 179–190.
doi:10.1007/s10765-005-2365-z

[31] Beechem, T., Graham, S., Kearney, S. P., Phinney, L. M., and Serrano, J. R., "Simultaneous Mapping and Stress in Microdevices Using Micro-Raman Spectroscopy," *Review of Scientific Instruments*, Vol. 78, No. 6, 2007, Paper 061301.
doi:10.1063/1.2738946